

# Grain growth control of isotope exchange between rocks and fluids

Michihiko Nakamura Institute of Mineralogy, Petrology, and Economic Geology, Graduate School of Science, Tohoku University, Aoba, Sendai 980-8578, Japan

Hisayoshi Yurimoto Division of Earth and Planetary Sciences, Hokkaido University, Sapporo 060-0810, Japan, and Department of Earth and Planetary Sciences, Tokyo Institute of Technology, Meguro, Tokyo 152-8551, Japan

E. Bruce Watson Department of Earth and Environmental Sciences, Rensselaer Polytechnic Institute, Troy, New York 12180, USA

## ABSTRACT

**Isotope exchange between fluid and rocks has been traditionally considered to be rate limited by two elementary processes: lattice diffusion in the matrix minerals and dissolution into the fluid followed by precipitation from it. In this study we show the results of high-pressure experiments on  $^{18}\text{O}$ -water infiltration into quartzite that point to a third, highly efficient process: grain growth accompanied by migration of the grain boundaries (GBs) that are isotopically enriched by GB diffusion and surface exchange. We predict on the basis of a mass-transfer mechanism discrimination diagram that this GB sweeping is the primary control on isotopic equilibration under hydrothermal conditions in various fine-grained rocks with low fluid fraction. Grain growth should be considered when interpreting and simulating isotope and chemical composition of rocks and fluids.**

**Keywords:** grain boundary, oxygen isotope, fluid flow, diffusion, quartzite.

## INTRODUCTION

Oxygen isotope records in rocks have been widely used to elucidate fluid-rock interaction processes. A specific process of isotope exchange needs to be assumed for estimating the isotope composition and flux of the fluid and the closure temperature for isotope thermometry (e.g., Eiler et al., 1993; Lewis et al., 1998). The processes generally assumed to be rate limiting during isotope and chemical exchange are lattice diffusion and dissolution-reprecipitation (e.g., Giletti, 1985; Criss et al., 1987; McConnell, 1995; Cole and Chakraborty, 2001). This assumption is, however, often difficult to test in natural rock samples because grain-scale isotope and chemical traces of fluids can be easily blurred by annealing and late-stage geologic events. Previous studies have shown that isotope exchange is enhanced in rock recrystallization through coarsening (Stoffregen, 1996; Zheng et al., 1999), exsolution (Farquhar and Chacko, 1994) and stress deformation (O'Hara et al., 1997), but the fundamental mechanisms of isotope exchange have been attributed to the two conventional processes. Wasson et al. (2001) proposed dissolution of high-energy grain boundary (GB) and immediate reprecipitation as a mechanism for rapid  $^{17}\text{O}$  enrichment at the rim of melilitite in the carbonaceous chondrites, although their mineralogical details remain uncertain. We investigated the mechanism of fluid-rock isotope exchange using hydrothermal experiments, where  $^{18}\text{O}$ -enriched water infiltrated into dry quartzite.

On the basis of micro-imaging of isotope distribution in the run products, grain growth accompanied by sweeping of GBs enriched in  $^{18}\text{O}$  is proposed as a dominant exchange mechanism. We then extend the experimental result to the other fluid-rock systems using a mass-transfer mechanism discrimination diagram.

## EXPERIMENTAL AND ANALYTICAL METHODS

Texturally equilibrated, dense quartzites with natural  $^{18}\text{O}$  abundance ( $^{18}\text{O} / \text{total O} = 0.20\%$ ) were presynthesized in a piston-cylinder apparatus from a mixture of amorphous silica and fine-grained quartz powder in Pt-lined Ni cylinders at 913 °C and 1.0 GPa; these were juxtaposed with reservoirs of silica-saturated water to form infiltration couples (Nakamura and Watson, 2001). We executed a series of infiltration experiments at 621–925 °C and 0.8 GPa where  $^{18}\text{O}$ -enriched (~96.2%) water was used. The aqueous fluid penetrated the quartzite grain edges, forming an interconnected network along grain triple junctions by dissolution and reprecipitation. The driving force for infiltration is the chemical potential gradient arising from the difference in quartz surface curvature at the infiltration front relative to that in regions already penetrated by fluid. The replacement of relatively high energy grain boundaries by lower-energy quartz fluid interfaces also reduces the overall free energy of the system. The fluid fraction in the infiltrated quartzite (measured

as porosity of the quenched run products) is <4 vol.%. The rate of grain growth in the infiltrated quartzite was dramatically enhanced. Grain growth is a process driven by interfacial energy reduction, and thus occurs inevitably in deep-seated rocks. With increasing temperature and run duration, the infiltration distance systematically increased. From the infiltration experiments with  $^{18}\text{O}$  water, we selected for secondary ion mass spectrometer (SIMS) analysis a typical run at 823 °C for 8 hr, where the infiltration distance is 800–900  $\mu\text{m}$  and mean grain size measured by intersection method increased from ~10  $\mu\text{m}$  to ~20  $\mu\text{m}$ .

The run products were observed by JEOL JSM-5310 scanning electron microscope (SEM) equipped with an Oxford mini-CL cathodoluminescence (CL) detector. The acceleration voltage was 15kV, and sample current was 3 nA for CL images. The  $^{18}\text{O}$  distribution in the quartzite was imaged semiquantitatively using a CAMECA ims-1270 SIMS with stacked CMOS-type active pixel sensor (SCAPS) at Tokyo Institute of Technology (Yurimoto et al., 2003). For isotope imaging, we used the positive 20keV Cs ions with 10 nA primary current. The oxygen secondary ions were accelerated to ~10 keV. To obtain a homogeneous distribution of the secondary ion emission, primary ions were rastered over an area of 90  $\times$  90  $\mu\text{m}$ , and the secondary ions generated from the central area (~60  $\times$  60  $\mu\text{m}$ ) were directly projected onto the image projection plane by stigmatic optics of the IMS-1270. Quantitative point analyses were also conducted using a focused primary beam, typically 4  $\mu\text{m}$  in diameter. A normal incidence electron gun was used for charge compensation. The primary ion beam was mass-filtered positive 20 keV Cs ions. The primary beam current was  $\approx$ 1 pA, adjusted to obtain a count rate of  $\approx$ 4  $\times$  10<sup>5</sup> cps for negative  $^{16}\text{O}$  ions. The mass resolution power was set to  $\approx$ 6000. Additional analytical procedures are described in Yurimoto et al. (1998, 2003).

## RESULTS

Figure 1 shows the  $^{18}\text{O}$  concentration and CL images of the run product. The  $^{18}\text{O}$  dis-

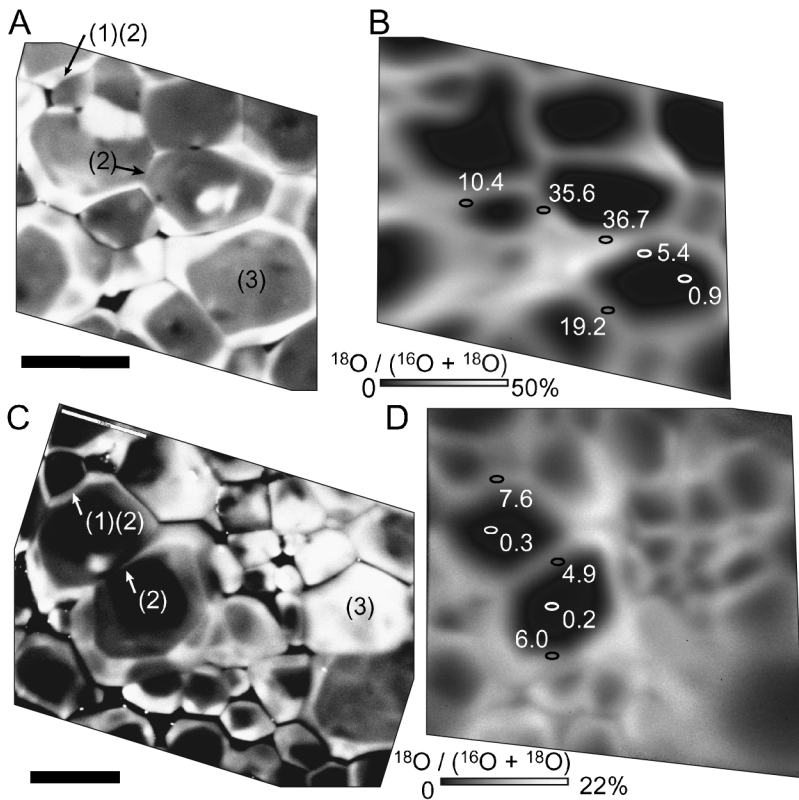


**Figure 1.** A, C: Cathodoluminescence (CL) images of quartzite after infiltration of  $^{18}\text{O}$  water at 823 °C for 8 h. B and D are oxygen-isotope micro-imagings of almost the same portions as in A and C, respectively.  $^{18}\text{O}$  distribution is virtually coincident with high CL-brightness area, showing that quartz swept by grain boundaries is enriched with  $^{18}\text{O}$ . Numbers in parentheses show examples of grain growth microstructures in text. Bright and dark spots in CL images, which do not correspond to the isotope distribution, are relicts of starting quartz powders. Spots for quantitative analyses are shown by ellipses with  $^{18}\text{O}$  contents. Scale bars, 20  $\mu\text{m}$ .

tribution and CL intensity, which are nearly coincident, display typical characteristics of grain growth microstructure as follows. (1) The high  $^{18}\text{O}$ -concentration and CL-intensity zones are thicker in the convex side of the present grain boundaries than in the opposite concave side. (2) The grain boundaries with relatively large curvature are accompanied by thick, high  $^{18}\text{O}$  and CL zones compared to those with small curvature. (3) Relatively large grains are outlined by a concave-outward  $^{18}\text{O}$ -rich rim, and small grains have a convex-outward  $^{18}\text{O}$ -poor rim. These observations show that the area swept by the migrated grain boundaries have high  $^{18}\text{O}$  concentration, because the GB migrates toward the concave side at a velocity proportional to its curvature (Kingery et al., 1976). We quantitatively confirmed the thickness of the  $^{18}\text{O}$ -enriched zone and its asymmetrical aspect relative to the grain boundaries by spot analysis (Fig. 2). On the convex side of the present grain boundaries, a high  $^{18}\text{O}$ -concentration zone (20–36%  $^{18}\text{O}$ ) of 3–5  $\mu\text{m}$  thickness is formed, and  $^{18}\text{O}$  enrichment (>1%) extends ~10  $\mu\text{m}$  from the present grain boundaries. In contrast, the concave side lacks a high  $^{18}\text{O}$ -

concentration zone, and the  $^{18}\text{O}$  enrichment extends <4  $\mu\text{m}$  into the grain. Such an asymmetrical feature and the sigmoidal profile of the  $^{18}\text{O}$  concentration in the convex side cannot be produced by lattice diffusion from a stationary GB. In Figure 2, a calculated diffusion profile of  $^{18}\text{O}$  concentration is shown for comparison. The diffusion calculation was made with surface  $^{18}\text{O}$  contents of 20 and 36% and a diffusion coefficient of  $2.4 \times 10^{-17} \text{ m}^2/\text{s}$  corresponding to the run temperature (Giletti and Yund, 1984). This is the value parallel to the c-axis, the fastest among the reported directions (Dennis, 1984). The water fugacity effect of 0.35 GPa, the highest reported experimental pressure, has also been incorporated into the diffusion coefficient. The measured  $^{18}\text{O}$  concentrations in the concave side may correspond with those calculated in lattice diffusion profiles within the uncertainty of the SIMS spot size, although the diffusion distances may be overestimated given that the GB is migrating. In the convex side, the  $^{18}\text{O}$ -enriched zone is clearly thicker than the lattice diffusion distance.

Having ruled out lattice diffusion as the primary means of  $^{18}\text{O}$  exchange, we investigated

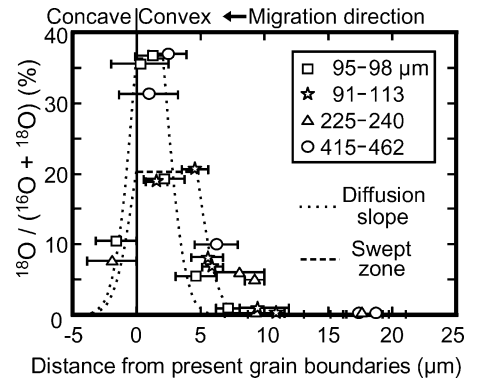


**Figure 2.**  $^{18}\text{O}$ -concentration profiles across present GBs by quantitative spot analyses. Distances from GBs to analyzed points were measured on SEM images after SIMS analysis. Numbers in legend are distances of analyzed positions from interface with fluid reservoir. Dotted lines show diffusion slopes calculated assuming boundary  $^{18}\text{O}$  concentrations of 20% and 36%. Dashed horizontal lines show concentration of swept zone. Horizontal bars represent SIMS spot size.

dissolution-precipitation as a possible mechanism of grain growth and consequent isotopic resetting. Dissolution of small grains with normal  $^{18}\text{O}$  abundance and subsequent precipitation of  $^{18}\text{O}$ -enriched quartz on the surface of the larger grains may proceed via the fluid network. In the present experiments, however, fluid penetrates only along grain edges (triple junctions) and corners, not in the two-dimensional boundaries between two grains, since the dihedral angle between quartz and fluid is ~60° (Watson and Brenan, 1987). SEM observations of both polished cross sections and the three-dimensional surface of the plucked grain surface support the absence of continuous fluid film at the grain boundaries of the quartzite.

Consequently, the observed  $^{18}\text{O}$  enrichment along the two-dimensional boundaries between two grains must be explained by a mechanism other than lattice diffusion and dissolution-precipitation. We propose that sweeping of GBs enriched in  $^{18}\text{O}$  is responsible for the formation of a high  $^{18}\text{O}$ -concentration zone at the concave side of quartzite GBs (Nakamura et al., 2001). The  $^{18}\text{O}$  is transported into the GBs mainly as molecular water (Farver and Yund, 1991) by GB diffusion, then exchanges with  $^{16}\text{O}$  at the quartzite GBs to attain surface equilibrium. The combination of the successive rapid processes, i.e., GB diffusion, surface reaction, and GB migration, may result in a larger exchange flux than lattice diffusion. The relative efficiency of lattice diffusion and GB sweeping is determined by the lattice diffusion coefficient and the GB migration rate, as discussed in the next section. The relative efficiency of dissolution-precipitation and GB sweeping depends on the proportion of

surface area of the quartz grains in direct contact with fluid. Assuming uniform grain size, the proportion in the experimental conditions is estimated at <30% on the basis of the geometrical calculation of German (1985). In the extreme case where an interconnected fluid network is absent, GB sweeping is likely to be the only effective means of fluid/rock equilibration as long as the GB diffusive flux is sufficient.

The atomic-level mechanism of isotope exchange in the grain boundaries is not well known. The quartz GB may be hydroxylated and a few monolayers of adsorbed water may be formed within 1 nm from the quartz surface (Parks, 1984). Breaking and reforming of silicon-oxygen bonds might be considered similar in its consequences to dissolution-precipitation. Molecular dynamics simulations of silicate minerals surfaces (Sakuma et al., 2003) show, however, that the water at the mineral surfaces is structured, having different physical properties from those of bulk water.

Diffusion of solute along the GBs of some metals and calcite can cause the GB motion in a phenomenon known as “chemically induced grain boundary migration” (CIGM; e.g., Cahn and Balluffi, 1979; Evans et al., 1986). CIGM results in asymmetrical chemical enrichment in the area swept by GBs, and the phenomenological diffusivity in migrating GBs can be several orders of magnitude higher than that of stationary GBs. In this sense, GB sweeping bears a striking resemblance to CIGM. In contrast to GB sweeping, however, CIGM increases the interfacial energy, and its driving force is generally considered to be coherency strain. The solute-metal systems that can cause CIGM are thus limited (Hay and Evans, 1987), and GB diffusion of isotope does not cause CIGM.

### EVALUATION OF THE DOMINANT MECHANISM

In order to evaluate the dominant mechanism that controls isotopic flux between fluid and rocks, we consider a mass conservation equation in one-dimensional two-phase flow,

$$\frac{\partial C_f}{\partial t} + \frac{\partial C_f}{\partial x} = Da(C_s - KC_f) \quad (1)$$

where  $C_f$  and  $C_s$  are isotope concentrations in fluid and solid, respectively,  $K$  is the solid/fluid isotopic fractionation coefficient,  $t$  is time, and  $x$  is the coordinate (Hauri, 1997). The Damköler number,  $Da$ , is a dimensionless parameter describing the rate of reaction relative to the rate of fluid flow in a reactive transport system. We can compare the lattice diffusion and GB sweeping in terms of the efficiency in isotopic flux by using the Damköler numbers for the two processes. In the case of GB sweeping-controlled exchange,

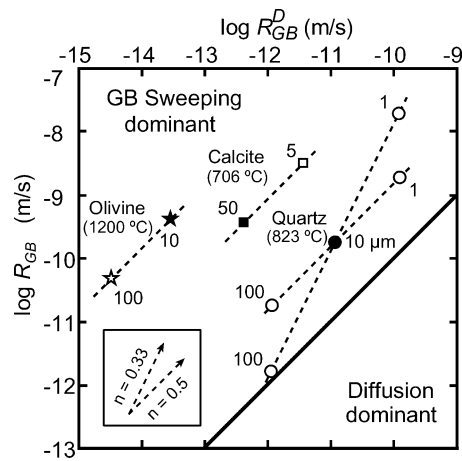


**Figure 3. Mass-transfer mechanism discrimination diagram showing relative efficiencies of lattice diffusion and GB sweeping.  $R_{GB}^D$  is GB migration rate that is equivalent in fluid-rock mass flux to lattice diffusion in one-dimensional two-phase flow. Dashed lines with slope = 1 and 2 represent grain size dependence for  $n = 0.5$  and  $0.33$ , respectively, where  $n$  is power of grain growth rate law [equation (3)]. Solid circle indicates data for oxygen-isotope exchange between water and quartzite with  $10 \mu\text{m}$  grain radius at  $823 \text{ }^\circ\text{C}$  (this study). Solid square represents a calcite aggregate with  $50 \mu\text{m}$  at  $706 \text{ }^\circ\text{C}$ . Grain growth data are from Covey-Crump (1997), where experimental pressure is  $185 \text{ MPa}$  and  $n = 0.5$ ; grain growth stopped when grain diameter reached  $97 \mu\text{m}$  by impurity pinning. Oxygen diffusion coefficient is from Farver (1994). Solid star represents an olivine aggregate with  $10 \mu\text{m}$  radius at  $1200 \text{ }^\circ\text{C}$ . Grain growth data are from Karato (1989), where experimental pressure is  $300 \text{ MPa}$  and  $n = 0.5$ ; oxygen diffusion coefficient from Ryerson et al. (1989). All experiments cited were executed under hydrothermal conditions. Open symbols with grain sizes are extrapolation from experimental data.**

the Damköler number can be written in the same form as for dissolution-precipitation, replacing the linear dissolution-precipitation rate with time-averaged GB migration rate,  $RL_{GB}$ . By equating the Damköler numbers for GB sweeping- and diffusion-controlled exchanges [equations (6) and (16) in Hauri (1997)], we can define the GB migration rate that is equivalent to lattice diffusion in terms of the isotope exchange flux,  $R_{GB}^D$ , as follows:

$$R_{GB}^D = 5 \frac{D_s}{a} \quad (2)$$

where  $D_s$  is the diffusion coefficient of the species of interest in the solid phase and  $a$  is the grain radius. For the experimental temperature and grain size ( $823 \text{ }^\circ\text{C}$ ,  $20 \mu\text{m}$ ),  $R_{GB}^D$  is calculated using the oxygen diffusion coefficient in quartz (Giletti and Yund, 1984) and plotted in Figure 3 against  $R_{GB}$ , the increase rate of the mean grain size. The measured  $R_{GB}$

( $\sim 0.5 \mu\text{m/hr}$ ) is  $10^2$  times larger than the calculated  $R_{GB}^D$ , confirming that GB sweeping is much more effective than lattice diffusion in terms of isotope exchange flux.

As indicated by equation (2),  $R_{GB}^D$  is inversely proportional to grain radius. To put the experimental results into the natural context of fluid-rock interaction, the effect of grain size on mass flux must be evaluated. Lacking explicit data for GB migration rates, we deduced the GB migration rate from a grain growth rate law. The grain growth rate law can be approximated by the following form when increases of grain radius are sufficiently large:

$$a = kt^n \quad (3)$$

where  $t$  is the duration of the growth period and  $k$  is the rate constant. The power  $n$  is assumed to be  $0.5$  for isotropic, pure, single-phase aggregates, and  $0.33$  for the cases where pinning of GB by second phase or impurities occurs (e.g., Covey-Crump, 1997). Since the average GB migration rate can be approximated by the growth rate of mean grain size,

$$R_{GB} = \frac{da}{dt} \propto a^{(1-1/n)}, \quad (4)$$

for  $n = 0.5$ , GB migration rate is inversely proportional to grain radius, and thus the relative efficiency of GB sweeping to lattice diffusion does not change with grain size (slope = 1 in Fig. 3). On the other hand, the relative efficiency decreases in proportion to  $1/a$  for  $n = 0.33$  (slope = 2). We assume that GB sweeping will govern oxygen isotope equilibration of quartzite with a radius of  $100 \mu\text{m}$  even if  $n = 0.33$ , as long as the grain growth rate law is valid. It has been reported that grain growth often ceases at a maximum grain size, probably due to pinning by impurities. Grain size is also suppressed by dynamic recrystallization under differential stress. Isotope exchange rate in natural rocks can thus be influenced by impurity and stress environments.

The GB sweeping mechanism will work not only for oxygen isotopes in quartz but also for other isotope and chemical constituents in rocks. Figure 3 may be used as a mass-transfer mechanism discrimination diagram for various fluid-rock interactions showing the relative efficiency of lattice diffusion and GB sweeping, with the data set of grain growth rate (GB migration rate) and the lattice diffusion coefficient of interest. Among the quite limited data set, the behavior of oxygen in calcite and olivine aggregates is plotted in Figure 3. As is the case with quartzite in this study, GB sweeping is expected to be much more effective than lattice diffusion in fine-grained calcite and olivine aggregates. Lattice diffusion should become more important in the coarser-



grained rocks where grain growth deviates from equation (3) and GB migrates very slowly due to impurity pinning. On the other hand, the dissolution-precipitation process becomes important when the contiguity of the fluid-bearing rock—i.e., the fraction of internal surface area of a mineral grain shared with other grains—is small; namely, when the dihedral angle is small and the fluid fraction is large. The grain growth rate, like the diffusion coefficient and the dissolution-precipitation rate, is a fundamental parameter controlling isotopic exchange, but it is one for which few experimental data are available. In the regime dominated by GB sweeping, it is the mineral with large grain growth rate, not that with large diffusivity, that undergoes effective isotopic and chemical exchange with fluid as long as GB diffusivity is large enough to attain surface isotopic equilibrium. The activation energies of the GB migration rates are considered to be close to those of the GB diffusion coefficient (Kingery et al., 1976) and thus smaller than those of the lattice diffusion coefficient. This would make the role of GB sweeping more significant among the isotope exchange mechanisms in low-temperature aqueous alteration.

The grain-scale  $\delta^{18}\text{O}$  zonings in minerals have been used as a source of information for fluid-rock interaction processes (e.g., Mora et al., 1999; Valley and Graham, 1996). Interpretation of the interaction history based on grain-scale zoning depends strongly on the assumed exchange mechanism. The GB sweeping mechanism results in a characteristic pattern such as fluid component-enriched zones with relatively steep gradient, as shown in Figures 1 and 2.

#### ACKNOWLEDGMENTS

We thank K. Nagashima, T. Kunihiro, and T. Yoshida for help in the laboratory, and D. Wark, K. Kawamura, T. Nagase, and T. Hiraga for discussion. J. Farver, W. Peck and an anonymous reviewer provided helpful reviews. This study was supported by Grant-in-Aid for Scientific Research to Nakamura and Yurimoto and by U.S. Department of Energy grant no. DE-FG02-94ER14432 to Watson.

#### REFERENCES CITED

Cahn, J.W., and Balluffi, R.W., 1979, On diffusional mass transport in polycrystals containing stationary or migrating grain boundaries: *Scripta Metallurgica*, v. 13, p. 499–502, doi: 10.1016/0036-9748(79)90077-2.

Cole, D.R., and Chakraborty, S., 2001, Rates and mechanisms of isotopic exchange, in Valley, J.W., and Cole, D.R., eds., *Stable isotope geochemistry, Reviews in mineralogy* 43: Washington, D.C., Mineralogical Society of America, p. 83–223.

Covey-Crump, S.J., 1997, The normal grain growth behavior of nominally pure calcite aggregates: *Contributions to Mineralogy and Petrology*, v. 129, p. 239–254, doi: 10.1007/s004100050335.

Criss, R.E., Gregory, R.T., and Taylor, H.P., Jr., 1987, Kinetic theory of oxygen isotopic ex-

change between minerals and water: *Geochimica et Cosmochimica Acta*, v. 51, p. 1099–1108, doi: 10.1016/0016-7037(87)90203-1.

Dennis, P.F., 1984, Oxygen self-diffusion in quartz under hydrothermal conditions: *Journal of Geophysical Research*, v. 89, p. 4047–4057.

Eiler, J.M., Valley, J.W., and Baumgartner, L.P., 1993, A new look at stable isotope thermometry: *Geochimica et Cosmochimica Acta*, v. 57, p. 2571–2583, doi: 10.1016/0016-7037(93)90418-V.

Evans, B., Hay, R.S., and Shimizu, N., 1986, Diffusion induced grain-boundary migration in calcite: *Geology*, v. 14, p. 60–63, doi: 10.1130/0091-7613(1986)14<60:DGMIK>2.0.CO;2.

Farquhar, J., and Chacko, T., 1994, Exsolution-enhanced oxygen exchange: Implications for oxygen isotope closure temperature in minerals: *Geology*, v. 22, p. 751–754, doi: 10.1130/0091-7613(1994)022<0751:EEOEIF>2.3.CO;2.

Farver, J.R., 1994, Oxygen self-diffusion in calcite: Dependence on temperature and water fugacity: *Earth and Planetary Science Letters*, v. 121, p. 575–587, doi: 10.1016/0012-821X(94)90092-2.

Farver, J.R., and Yund, R.A., 1991, Oxygen diffusion in quartz: Dependence on temperature and water fugacity: *Chemical Geology*, v. 90, p. 55–70, doi: 10.1016/0009-2541(91)90033-N.

German, R.M., 1985, The contiguity of liquid phase sintered microstructures: *Metallurgical Transactions A*, v. 16A, p. 1247–1252.

Giletti, B.J., 1985, The nature of oxygen transport within minerals in the presence of hydrothermal water and the role of diffusion: *Chemical Geology*, v. 53, p. 197–206, doi: 10.1016/0009-2541(85)90069-5.

Giletti, B.J., and Yund, R.A., 1984, Oxygen diffusion in quartz: *Journal of Geophysical Research*, v. 89, p. 4039–4046.

Hauri, E.H., 1997, Melt migration and mantle chromatography, 1: Simplified theory and conditions for chemical and isotopic decoupling: *Earth and Planetary Science Letters*, v. 153, p. 1–19, doi: 10.1016/S0012-821X(97)00157-X.

Hay, R.S., and Evans, B., 1987, Chemically induced grain boundary migration in calcite: Temperature dependence, phenomenology, and possible applications to geologic systems: *Contributions to Mineralogy and Petrology*, v. 97, p. 127–141, doi: 10.1007/BF00375220.

Karato, S., 1989, Grain growth kinetics of olivine aggregates: *Tectonophysics*, v. 168, p. 255–273, doi: 10.1016/0040-1951(89)90221-7.

Kingery, W.D., Bowen, H.K., and Uhlmann, D.R., 1976, *Introduction to ceramics* (second edition): New York, Wiley, 1056 p.

Lewis, S., Holness, M., and Graham, C., 1998, Ion microprobe study of marble from Naxos, Greece: Grain-scale fluid pathways and stable isotope equilibration during metamorphism: *Geology*, v. 26, p. 935–938, doi: 10.1130/0091-7613(1998)026<0935:IMSOMF>2.3.CO;2.

McConnell, J.D.C., 1995, The role of water in oxygen isotope exchange in quartz: *Earth and Planetary Science Letters*, v. 136, p. 97–107, doi: 10.1016/0012-821X(95)00198-L.

Mora, C.I., Riciputi, L.R., and Cole, D.R., 1999, Short-lived oxygen diffusion during hot, deep-seated meteoric alteration of anorthosite: *Science*, v. 286, p. 2323–2325, doi: 10.1126/science.286.5448.2323.

Nakamura, M., and Watson, E.B., 2001, Experimental study of aqueous fluid infiltration into quartzite: Implications for the kinetics of fluid

redistribution and grain growth driven by interfacial energy reduction: *Geofluids*, v. 1, p. 73–89, doi: 10.1046/j.1468-8123.2001.00007.x.

Nakamura, M., Yurimoto, H., and Watson, E.B., 2001, Rapid oxygen-isotope exchange between fluid and synthesized quartzite: Insights from CL and SIMS-SCAPS study: Houston, Texas, Lunar and Planetary Institute, LPI Contribution 1088, 11th Annual V.M. Goldschmidt Conference, CD-ROM, Abstract 3216.

O'Hara, K.D., Sharp, Z.D., Moecher, D.P., and Jenkin, G.R., 1997, The effect of deformation on oxygen isotope exchange in quartz and feldspar and the significance of isotopic temperatures in mylonites: *Journal of Geology*, v. 105, p. 193–204.

Parks, G.A., 1984, Surface and interfacial free energies of quartz: *Journal of Geophysical Research*, v. 89, p. 3996–4008.

Ryerson, F.J., Durham, W.B., Cherniak, D.J., and Lanford, W.A., 1989, Oxygen diffusion in olivine: Effect of oxygen fugacity and implications for creep: *Journal of Geophysical Research*, v. 94, p. 4105–4118.

Sakuma, H., Tsuchiya, T., Kawamura, K., and Otsubo, K., 2003, Large self-diffusion of water on brucite surface by ab initio potential energy surface and molecular dynamics simulations: *Surface Science*, v. 536, p. L396–L402, doi: 10.1016/S0039-6028(03)00577-6.

Stoffregen, R., 1996, Numeric simulation of mineral-water isotope exchange via Ostwald ripening: *American Journal of Science*, v. 296, p. 908–931.

Valley, J.W., and Graham, C.M., 1996, Ion microprobe analysis of oxygen isotope ratios in quartz from Skye granite: Healed microcracks, fluid flow, and hydrothermal exchange: *Contributions to Mineralogy and Petrology*, v. 124, p. 225–234, doi: 10.1007/s004100050188.

Wasson, J.T., Yurimoto, H., and Russell, S.S., 2001,  $^{16}\text{O}$ -rich melilite in CO3.0 chondrites: Possible formation of common,  $^{16}\text{O}$ -poor melilite by aqueous alteration: *Geochimica et Cosmochimica Acta*, v. 65, p. 4539–4549, doi: 10.1016/S0016-7037(01)00738-4.

Watson, E.B., and Brenan, J.M., 1987, Fluids in lithosphere, 1. Experimentally determined wetting characteristics of  $\text{CO}_2$ - $\text{H}_2\text{O}$  fluids and their implications for fluid transport, host-rock physical properties, and fluid inclusion formation: *Earth and Planetary Science Letters*, v. 85, p. 497–515, doi: 10.1016/0012-821X(87)90144-0.

Yurimoto, H., Ito, M., and Nagasawa, H., 1998, Oxygen isotope exchange between refractory inclusion in Allende and solar nebula gas: *Science*, v. 282, p. 1874–1877, doi: 10.1126/science.282.5395.1874.

Yurimoto, H., Nagashima, K., and Kunihiro, T., 2003, High precision isotope micro-imaging of materials: *Applied Surface Science*, v. 203–204, p. 793–797, doi: 10.1016/S0169-4332(02)00825-5.

Zheng, Y.-F., Satir, M., Metz, P., and Sharp, Z.D., 1999, Oxygen isotope exchange processes and disequilibrium between calcite and forsterite in an experimental C-O-H fluid: *Geochimica et Cosmochimica Acta*, v. 63, p. 1781–1786, doi: 10.1016/S0016-7037(99)00127-1.

Manuscript received 26 February 2005  
 Revised manuscript received 28 June 2005  
 Manuscript accepted 29 June 2005

Printed in USA